Monthly Notices of the ROYAL ASTRONOMICAL SOCIETY
MNRAS **497,** 3142–3148 (2020) doi:10.1093/mnras/staa2141

Detection of very-high-energy gamma-ray transients with monitoring facilities

G. La Mura,[1]★ G. Chiaro,[2] R. Conceição,[1,3] A. De Angelis,[4,5,6] M. Pimenta[1,3] and B. Tomé[1,3]

[1]*Laboratório de Instrumentação e Física Experimental de Partículas (LIP), Av. Prof. Gama Pinto 2, PT-1649-003 Lisboa, Portugal*
[2]*Istituto di Astrofisica Spaziale e Fisica Cosmica (IASF-INAF), Via A. Corti 12, I-20133 Milano, Italy*
[3]*Instituto Superior Técnico (IST), Av. Rovisco Pais 1, PT-1049-001 Lisboa, Portugal*
[4]*Dipartimento di Fisica e Astronomia - Università di Padova, Via Marzolo 8, I-35131 Padova, Italy*
[5]*Dipartimento di Scienze Matematiche, Informatiche e Fisiche - Università degli Studi di Udine, Via Palladio 8, I-33100 Udine, Italy*
[6]*Istituto Nazionale di Fisica Nucleare sez. Padova (INFN), Via Marzolo 8, I-35131 Padova, Italy*

Accepted 2020 July 17. Received 2020 June 18; in original form 2020 January 13

ABSTRACT

The observation of very-high-energy γ-rays (VHE γ-rays, $E > 100$ GeV) has ledto the identification of extremely energetic processes and particle-acceleration sites both within our Galaxy and beyond. It is expected that VHE facilities, such as the Cherenkov Telescope Array, will explore these sources with an unprecedented level of detail. However, the transient and unpredictable nature of many important processes means that their observation requires the development of proper monitoring strategies. In this study, we estimate the properties of VHE transients that can be effectively detected by monitoring facilities. We use data collected by the *Fermi*-LAT instrument during its monitoring campaign to select events that are probably associated with VHE emission. We use this sample to estimate the frequency, the luminosity and the time-scales of various transients, focusing on blazar flares and gamma-ray bursts. We discuss how the balance between the field of view, sensitivity and duty cycle of an observatory affects the likelihood of detecting transients that occur at the inferred rates, and we conclude by describing the contribution that current and near-future monitoring facilities can make to the identification and study of VHE transient emission.

Key words: instrumentation: detectors – galaxies: active – gamma-rays: general – gamma-ray bursts.

1 INTRODUCTION

The recent detection of a gamma-ray burst (GRB) associated with a gravitational wave event (GW170817, Abbott et al. 2017a,b) and of a flaring blazar consistent with the direction of an ultra-relativistic neutrino (TXS 0506+056, IceCube Collaboration 2018) demonstrated the importance of γ-ray monitoring in the identification of multi-messenger events. In both cases, the existence of an electromagnetic counterpart to the signals was first identified by γ-ray instruments, namely the Gamma-ray Burst Monitor (GBM, Meegan et al. 2009) for the neutron star merger originating GW170817, and the Large Area Telescope (LAT, Atwood et al. 2009) for the blazar flare associated with IceCube-170922A, with both instruments carried by the *Fermi Gamma-ray Space Telescope*. Follow-up observations executed at different wavelengths led to the clarification of other important characteristics, such as the identification of the GRB counterpart as a *kilonova* (e.g. Cowperthwaite et al. 2017), as well as the redshift and, hence, the distance and the luminosity of the processes (Blanchard et al. 2017; Paiano et al. 2018). In particular, the blazar TXS 0506+056 was detected at very high energy (VHE, $E \geq 100$ GeV) for the first time by the Major Atmospheric Gamma-ray Imaging Cherenkov (MAGIC) telescopes, shortly after the *Fermi* outburst (Mirzoyan 2017).

Detecting VHE photons from sources such as blazars and GRBs has several important implications. For example, the emission of VHE radiation and its association with the production of ultra-relativistic particles is a strong hint that these sources act as cosmic particle accelerators, and the interaction of γ-rays with the lower-energy photon field, forming the extragalactic background light (EBL), is an extremely powerful tool with which to constrain the effects of star formation and active galactic nuclei (AGNs) on cosmological evolution. During its long monitoring campaign, the *Fermi*-LAT telescope has firmly identified AGNs – blazars in particular – and GRBs as the most powerful extragalactic sources of photons above 10 GeV (Ajello et al. 2017, 2019). Some AGNs are known to have energy spectra that extend up to several teraelecton-volts, while the combination of observed GRB spectra and the identification of reliable counterparts at measurable redshifts suggested that GRBs could be intrinsically able to produce photons well above $E = 100$ GeV. This expectation would eventually be confirmed by the MAGIC and High Energy Stereoscopic System (HESS) observations of some GRBs (Mirzoyan 2019; Abdalla et al. 2019; MAGIC Collaboration 2019).

In recent times, our ability to observe VHE sources has greatly improved, thanks to the construction of large ground-based observatories using either the Imaging Atmospheric Cherenkov Telescope approach (IACT, such as HESS, MAGIC and the Very Energetic

★ E-mail: glamura@lip.pt

Radiation Imaging Telescope Array System VERITAS, Aharonian et al. 2006; Aleksić et al. 2016; Holder et al. 2008) or an Extensive Air Shower detector array (EAS, such as the High Altitude Water Cherenkov HAWC and the Large High Altitude Air Shower Observatory LHAASO, DeYoung 2012; Di Sciascio & LHAASO Collaboration 2016). Owing to the importance of VHE observations for our understanding of the physics of relativistic jets and light propagation through the Universe, great efforts are currently under way to improve the characteristics of these observatories. We can expect that the upcoming Cherenkov Telescope Array (CTA, CTA Consortium 2019) will achieve outstanding performance in this field. However, although the CTA will be able to observe the VHE sky at an unprecedented level of detail, its ability to perform regular monitoring of sources, to map vast regions of the sky and to promptly respond to fast transients will be strictly limited by its narrow field of view and its duty cycle. Furthermore, while dedicated monitoring programs, such as the one carried out by the First Geiger-mode Avalanche photo-diode Cherenkov Telescope (FACT, Anderhub et al. 2013), can cover a list of selected targets and, possibly, provide transient follow-up capabilities, the necessary observational requirements imply unavoidable gaps in the data flow. Therefore, the presence of survey instruments that continuously scan wide areas of the sky, like *Fermi*, is essential for the study of transient phenomena. Unfortunately, it is hard to maintain long-term survey missions in space, moreover the limited size of space-borne detectors implies a reduced efficiency in the VHE domain. It has been proposed that the observational coverage and continuity problems could be overcome using the wide field of view (FoV) of EAS facilities.

In this work, we use γ-ray monitoring data to study the distribution of transients that are more likely to be associated with VHE emission. We analyse the properties of these events and we compare them with the performance of instruments used to monitor or follow up transients. The paper is structured as follows: in Section 2, we use *Fermi*-LAT data to study the distribution of events that are known or predicted to produce VHE emission at a detectable level for CTA, describing our selection and assumptions and the implications; in Section 3, we discuss the possibilities that EAS arrays have to contribute to VHE transient monitoring; in Section 4, we compare different instruments and approaches; and, finally, in Section 5, we give our conclusions.

2 SELECTION OF VHE GAMMA-RAY TRANSIENTS

VHE transients are a fundamental probe of multi-messenger astrophysics and particle physics, but, at present, very little is known about the rate and the properties of these events. Because the performance of VHE instruments will have a critical impact on our ability to explore these events, we carry out a systematic study to assess how monitoring facilities can contribute to the investigation of them, by taking into account the source positions in the sky, their redshift, and the time-scales on which they can be detected. We develop this analysis in a sequence of steps that, starting from the available data, leads us to infer what instrument characteristics are required and what performances can be achieved. As a starting point, we use *Fermi*-LAT monitoring data to select a sample of transients that led to high-energy emission and are most likely connected with VHE activity. We use the fact that some of these transients are associated with sources that have already been detected at VHEs, suggesting that their spectra are not subject to severe cut-offs. Finally, we compare the selected data and our assumptions with the performance of various observing facilities, demonstrating that instruments with optimized monitoring capabilities can both act as effective alert systems and explore a spectral window that would otherwise be very difficult to monitor.

2.1 The spectrum of sources

We want to determine the distribution and the properties of the most important extragalactic VHE sources. To achieve this, we need to use a model that can be compared with observational data. In general, we can express the VHE photon spectrum observed from an astrophysical source at redshift z in the form

$$\frac{\mathrm{d}N(E)}{\mathrm{d}E} = N_0 \left(\frac{E}{E_0}\right)^{-[\alpha+\beta\log(E/E_0)]} \mathrm{e}^{-[\tau_E(z)+E/E_{\mathrm{c.o.}}]} \left[\mathrm{GeV}^{-1}\,\mathrm{cm}^{-2}\,\mathrm{s}^{-1}\right], \quad (1)$$

where α is the photon index ($\alpha \geq 1.5$ for most astrophysical sources), β is the curvature parameter ($\beta = 0$ for a pure power-law spectrum), E_0 is a scaling energy, $E_{\mathrm{c.o.}}$ is the cut-off energy, and $\tau_E(z)$ is the Universe opacity at energy E as a function of redshift.

Equation (1) implies that the number of photons available at energies $E \gg E_0$ can quickly become lower than 1 photon every few square metres. This means that instruments with small collecting areas, like those carried by satellites, require long observing times to characterize the high-energy spectra of sources and that they may not be able to effectively detect the highest-energy emission of a short time-scale event. Thanks to the long duration of the *Fermi*-LAT monitoring campaign, however, we are able to select a sample of sources, among those that were detected at high energy (HE, $E > 10$ GeV), and study their flaring activity.

2.2 AGN flares

Because most EBL models predict that the Universe optical depth for γ-ray photons with $E \simeq 1$ TeV is $\tau_{1\mathrm{TeV}} \geq 1$ already at $z \approx 0.1$ (Desai et al. 2019), it turns out that the study of photons with $E < 1$ TeV is critical to constrain EBL properties. However, while we know a handful of extragalactic sources that feature a persistent teraelectronvolt emission, the vast majority of VHE sources are characterized by generally unpredictable activity.

To study the distribution of VHE flaring sources, we undertook an analysis aimed at characterizing the frequency, the duration, and the possible spectral features of VHE AGN flares. We used the Second *Fermi*-LAT All-Sky Variability Analysis (2FAV, Abdollahi et al. 2017)[1] as a starting point to select a uniform sample of γ-ray flares. Because the second version of the catalogue includes 7.4 yr of variability analysis, with tools designed to inspect the γ-ray light-curves of specific sky areas and the possibility of extracting preliminary spectral fits to the soft (100–800 MeV) and the hard (0.8–300 GeV) LAT bands, we are able to search the LAT data for the brightest outbursts detected on a weekly time-scale. We therefore selected AGNs that have been associated with γ-ray flares and were detected with an energy flux greater than 10^{-12} erg cm^{-2} s^{-1} above 10 GeV in the Third Catalogue of Hard *Fermi*-LAT sources (3FHL, Ajello et al. 2017). This selection led to the identification of 160 sources, which have been associated with 2367 γ-ray flares, detected in the 2FAV hard band.

Although using the *Fermi*-LAT variability analysis to study the properties of flares has some limitations, we can identify examples of flares that triggered specific follow-up analysis. A comparison of 2FAV-selected flares with almost simultaneous analyses of data

[1] https://fermi.gsfc.nasa.gov/ssc/data/access/lat/FAVA/

suggests that the power-law fits to the 2FAV hard band give reasonable representations of the spectral energy distribution (SED). In general, flares are associated with spectral indexes that are harder than those that characterize the average SEDs of the 8-yr data set of the Fourth *Fermi*-LAT Gamma-ray Catalogue (4FGL, Fermi-LAT Collaboration 2020). While this procedure can effectively identify the events with the strongest HE activity, the extrapolation of spectra towards the VHE domain is subject to some degree of uncertainty, because sources may exhibit intrinsic spectral cut-offs. These, however, are not expected to be found below an energy of approximately 300 GeV. Indeed, some objects associated with our flare sample are detected by *Fermi*-LAT above 100 GeV, although several years of monitoring were necessary to collect the required statistics. In addition, many of the sources that exhibited the brightest flares have been detected at VHEs by IACT facilities (Wakely & Horan 2008), suggesting that intrinsic spectral cut-offs are unlikely to occur below 500 GeV. Therefore, in general, we do not expect severe cut-offs in flaring states, for which, on the contrary, many studies point to the existence of possible additional emission components (HESS Collaboration 2017; Prince, Majumdar & Gupta 2017; Zacharias et al. 2019), while it is well established that the blazar TXS 0506+056 was first detected in the VHE domain after being identified as a LAT flaring blazar consistent with an IceCube neutrino event (Abeysekara et al. 2018).

The selected data describe observations under the effect of the EBL opacity. Therefore, we can use the spectral parameters inferred from the variability analysis to estimate the flux produced by flaring sources in the VHE domain. To do this, we apply the EBL absorption model of Domínguez et al. (2011) to the extrapolation of equation (1) to $E > 100$ GeV and we use the resulting fluxes to select flaring events, which are estimated to be brighter than 4.40×10^{-12} erg cm^{-2} s^{-1} between 100 and 200 GeV, roughly corresponding to the limiting flux for a 5σ detection with CTA South (CTA-S) in 1 hr of observation. This further limitation leads to the selection of 1374 flares that were associated with AGNs in 7.4 yr of monitoring, and, thus, to an average flare rate of 187 events per year that increased the flux at a detectable level for a time-scale of 1 week. Following this method, we obtain a list of transients that CTA-S would be able to detect if every event lasted for exactly 1 week, with a flux constantly equal to its average value, as computed on a fixed time-binning, and provided that the target could be observed for 1 hr during the transient. In a more realistic scenario, the flaring activity is not limited to a smooth increase up to a constant luminosity, but it can include shorter features that show increases in flux of a factor of 3 over 1 d, and, more rarely, reach peaks of nearly 10 times the average for a few hours. Adopting these assumptions on the internal evolution of our sample of flares and assuming a Poissonian distribution to account for the underlying uncertainty, we can estimate that a total of 963 events may have led to a transient that would be brighter than our limiting flux for a few days (corresponding to an average rate of 130 ± 12 per year) and 237 to one that would have been detectable for a few hours (corresponding to an average rate of 32 ± 6 per year). Considering the duration of the monitoring campaign, we can therefore expect that VHE transients occur with the average rates shown in Fig. 1.

2.3 Gamma-ray bursts

At present, the data that we possess on the VHE properties of GRBs are still very scarce, and any attempt to model them is subject to large uncertainties, as a result of the many important free parameters

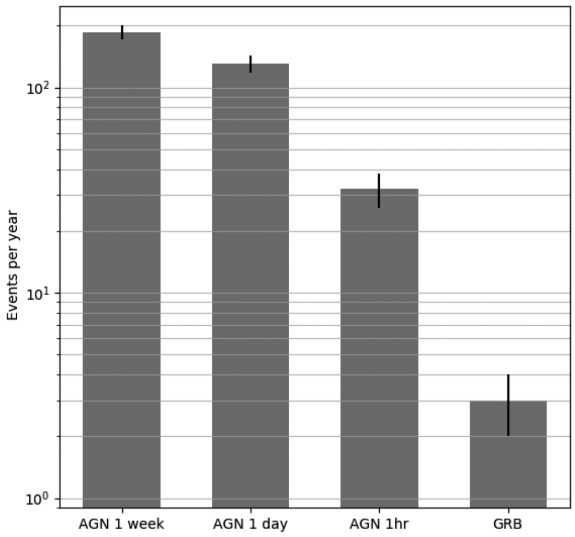

Figure 1. The estimated frequency of VHE transients associated with AGN flares of different duration and with GRBs. The events taken into account are limited to the ones that are expected to be bright enough to be detected by CTA-S if they are located within 20° of zenith and could be observed for 1 hr.

that affect the predicted luminosities and spectra (Galli & Piro 2008; Bernardini et al. 2019). If we are interested in an estimate of the rate of VHE events, we can start from the observation that GRBs detected with a maximum photon energy above 100 GeV are brighter towards the lower energy limit. As a consequence, we expect that GRBs with a significant VHE emission should in principle be detected by *Fermi*-LAT in the HE domain, if it is properly pointed.

According to the data presented in the second catalogue of LAT-detected GRBs (Ajello et al. 2019), in 10 yr of operation, the LAT has been able to detect 169 GRBs with photons above 100 MeV, while only 15 events were associated with photons detected above 10 GeV. By normalizing the detection rates with respect to the LAT effective area inferred from the P8R3_TRANSIENT_V2 instrument response function (IRF), and assuming an isotropic distribution of GRBs, we can relate the different detection rates to the probability that a specific GRB spectrum extends above a critical energy. If $N_{\rm GRB}(E)$ denotes the cumulative number of events per year that emit photons up to energy E and we assume an isotropic GRB distribution, we can reproduce the observed GRB rate from a power-law distribution in the form

$$N(E) = 291 \left(\frac{E}{100\,\mathrm{MeV}} \right)^{-1.5}. \quad (2)$$

Clearly, a simple extrapolation of the observed LAT trend is still a very limited approximation of the real GRB properties, because the reduced sensitivity of the LAT above 100 GeV and the extreme rarity of the most energetic photons can lead to a poor sampling of the actual HE properties. However, the emission of VHE photons requires favourable energetic conditions in the source, and, because the EBL opacity limits their propagation to within a relatively small horizon, we can expect that a rate of at least 3 ($\pm$2) GRBs per year may be associated with detectable VHE emission (see Fig. 1).

3 VHE TRANSIENT EVENT MONITORING

From our study of *Fermi*-LAT γ-ray transients, we estimated that several hundred transient events could represent high-priority targets for sub-TeV VHE investigations every year. Their unpredictable

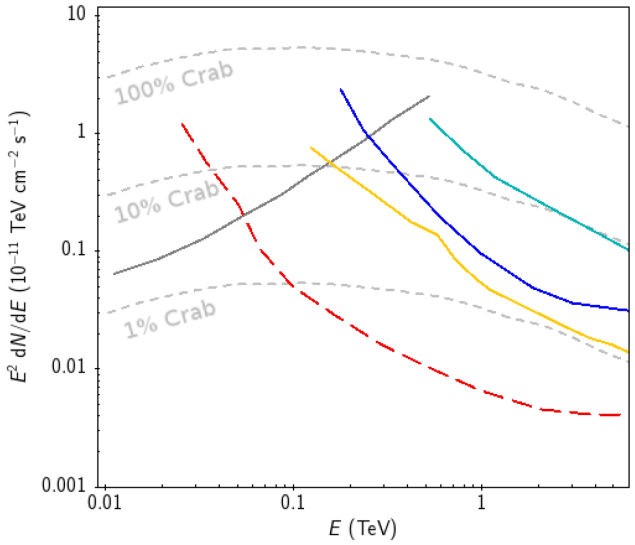

Figure 2. Differential sensitivity to a point-like source for HAWC (cyan continuous line), LHAASO (blue line) and SWGO (yellow line) as compared with the *Fermi*-LAT Pass 8 sensitivity (dark grey line) computed on 1 yr of observations. For comparison, the plot also shows different fractions of the Crab Nebula flux spectrum (short-dashed, light-grey curves), as well as the sensitivity achieved by CTA-S in 50 hr of observation (long-dashed red line).

nature and the possibility that a significant fraction of triggers issued by lower-energy monitoring instruments may have little or no VHE emission, however, raises the question of what instrument performance is required to identify the most relevant events. While CTA is obviously expected to provide the best sensitivity in this energy range, the performance of monitoring instruments on short time-scales is still very limited. *Fermi*-LAT has low sensitivity to VHE photons, while the largest ground-based facilities of HAWC and LHAASO are located in the Northern hemisphere and therefore do not provide full-sky coverage.

VHE particles – either cosmic rays or photons – that interact with the atmosphere generate a shower of relativistic secondary products, including charged particles and Cherenkov radiation, which develops downwards, approximately in the direction of the incoming primary. These showers can be tracked by collecting the Cherenkov light and by detecting the secondary particles that reach the ground. Arrays of particle detectors, placed on the ground but at high altitude, can infer the direction and the energy of atmospheric showers, provided that they are able to determine with sufficient accuracy the location, the arrival time and the energy carried by the secondary charged particles that reach them. For this work, we took the yellow curve in Fig. 2 as the reference curve for the Southern Wide field of view Gamma-ray Observatory[2] (SWGO, Schoorlemmer 2019). This curve was for the most part obtained through a straw-man model that assumed a facility based on water Cherenkov detectors (WCDs) covering an area of 80 000 m^2 with an 80 per cent filling factor (Albert et al. 2019). For the lower energies, below 300 GeV, the most important region of energy for this work, the assumed sensitivity is based on an end-to-end simulation (performed with GEANT4, Agostinelli et al. 2003) of a detector concept, which combines a WCD with white reflective walls and a resistive plate chamber (RPC), to effectively lower the energy threshold (Assis et al. 2018). The success of this concept relies on the ability of the WCDs to trigger on low-energy secondary photons while being able to measure time with a resolution better than 2 ns, which is crucial for a good geometrical reconstruction. The instrument performances illustrated in Fig. 2 are computed for a steady point-source located at a zenith distance of 20^o and under the assumption that it can be observed for 6 hr per day. For wide FoV instruments, we need to correct this sensitivity according to the visibility of different sky areas.

3.1 Sensitivity across the field of view

Although a wide-FoV instrument can simultaneously track targets located in different regions of the sky, the corresponding sensitivity depends on the zenith distance of every source. Owing to computational limitations, the dependence of the sensitivity on the shower inclination was obtained using the amount of shower electromagnetic energy at the ground as a proxy. This allowed us to use the shower simulations generated with CORSIKA (Heck et al. 1998), while skipping the full detector simulation and the application of the shower reconstruction analyses, as described in detail in Assis et al. (2018). While this is a crude estimate, we believe it is a conservative approach. On the one hand, the trigger probability decreases with increasing zenith angle, as fewer particles (energy) reach the ground owing to the increasing atmospheric thickness. On the other hand, the shower is spread over more of the array, which eases the geometric reconstruction. This not only has an impact on the astrophysical source position determination but also effectively reduces the hadronic background.

Because the Earth's daily rotation induces a transit that changes the fraction of time that a source spends at a specific zenith distance θ, depending on the latitude of the observing site and the source's declination, we derived the fraction of time $\Delta t(\theta)$ that every point in the sky spends at a given zenith distance θ, according to its declination. If an instrument operates for an observing time Δt, under conditions that change with time, like θ for a transiting source, the sensitivity of the observation scales as

$$S(\Delta t) = \left[\frac{1}{T_0}\sum_i \frac{\Delta t_i}{S_i^2(T_0)}\right]^{-1/2}, \qquad (3)$$

where Δt_i are the amounts of time during which we can consider the instrument to have a regular performance, while T_0 and $S_i(T_0)$ represent, respectively, the standard time interval, on which the sensitivity is computed, and the sensitivity under constant observing conditions over such an interval.

To derive the effective sensitivities that would result from the combined operation of LHAASO and SWGO observatories, we used the corresponding sensitivity curves, computed for 1 yr of observations, assuming that SWGO is located at a latitude of 23^{o}S.[3] We subdivided the sky into 2^o-wide strips of constant declination, and we computed the fraction of time that a point belonging to each of these strips spends at a zenith distance $\theta \leq 50^o$. We used the sensitivities computed as a function of θ for an energy of 300 GeV (Assis et al. 2018) to obtain the sensitivity degradation resulting when the zenith distance increases from $\theta = 0^o$ to $\theta = 50^o$ in steps of 5^o. Finally, we applied equation (3) to extract the sensitivity that an observation can effectively achieve

[2] www.swgo.org

[3] This is the latitude of the ALMA site, one of the possible candidate sites for such an experiment.

in the whole FoV, thus deriving an estimate of the limiting flux to detect a target within the monitored area. The result of this calculation, carried out for the SWGO and LHAASO experiments, is shown in Fig. 3, together with the distribution of VHE flaring AGNs.

4 COMPARISON BETWEEN EXPERIMENTS

Taking the performance of CTA-S[4] as the reference, our analysis of the *Fermi*-LAT monitoring data led to the identification of 160 blazars and of a fraction of GRBs, distributed across the whole sky, whose light-curves show transient VHE emission that is strong enough for detection in 1 hr of observation. Because blazars are sources of potential VHE activity for which we know the position in the sky, we can compare their emission with the predicted sensitivity of monitoring instruments that regularly scan the sky, such as LHAASO and SWGO, as illustrated in Fig. 3. The shaded areas represent the FoV covered within 50° of zenith, with a colour scale that illustrates the sensitivity degradation towards different sky regions, with respect to a target that culminates at the zenith. Only the instrument with the best estimated sensitivity is plotted in the overlap region.

If we apply an extrapolation of equation (1) to the spectra of the HE flares identified in our sample, taking into account the effects of EBL (Domínguez et al. 2011; Kudoda & Faltenbacher 2017), we can compare the predicted VHE fluxes with the chances that a monitoring instrument has to detect a specific transient. With the assumed instrument performance, it turns out that 21 blazars out of 160, listed in Table 1, showed a flaring activity that is comparable to the detection threshold of monitoring facilities (green symbols in Fig. 3). Eight of these sources, marked as stars in Fig. 3 and listed in bold-face in Table 1, have a predicted spectrum that is significantly brighter than the limiting flux expected for the instrument covering their location in the sky, or, in the case of MRK 421 and MRK 501, have already been detected by HAWC, while six of them appear in the *TeVCat*, which provides a list of objects that have already been detected in the VHE domain. The remaining sources, in contrast, show an estimated flaring activity that is too faint for detection by a monitoring instrument. All of these objects, however, remain of potential interest, because most of them have been associated with multiple flares, and the use of their averaged spectral properties can smear out the possible existence of sharp peaks in their light-curves at shorter time-scales.

Indeed, the successful operation of efficient monitoring instruments improves the chances of detecting and tracking flaring activity. CTA, with an observing budget of 1500 hr per year per site, corresponding to a duty cycle smaller than 20 per cent (Actis et al. 2011), and on the assumption that it can collect observational data for on average 5 hr per night, covering a FoV with an angular radius of 2°, has practically a null chance of being in place when a flare occurs. Assuming that CTA follows a scheduled observing plan (i.e. not taking into account Target of Opportunity observations), the probability of detecting a transient at a random position of the observable sky is proportional to the rate of the transient and to the ratio between the area covered by CTA observations and the total visible sky (approximately 2 sr, below 1 TeV). Recalling that our estimates of transient rates are based on the events that are bright enough to be detected in 1 hr of observation, and assuming that CTA exposures have no significant overlap above 1 hr, the scanned area increases with the duration of the flare, resulting in a higher detection chance for longer transients. Clearly, the detection probability could be even higher, if CTA were alerted to the occurrence of a transient, with accurate positional information. At present, however, the available instruments are not able to filter which low-energy transients will actually be associated with VHE emission, and following all the possible triggers would probably result in a high rate of false alarms.

Conversely, if we focus our attention on the sky region that will be covered by CTA-S, because of its better performance, we can illustrate the role of a monitoring facility by looking at the predicted detection rates illustrated in Fig. 4. If we use the results of our analysis to infer the average rate of transients with detectable VHE emission, applying visibility and duty-cycle constraints, we can expect that CTA will be able to detect dozens of transients per year with just 1 hr of observation, if every VHE event is associated with an accurate positional trigger. The number of potentially detectable sources is naturally expected to decrease for events with a shorter time-scale, and to drop practically to zero in the absence of a trigger. At present, the largest set of monitoring data in the HE domain is that provided by the *Fermi*-LAT, but even this information can only be accessed after a time lag of approximately 6 hr, owing to data down-link and processing requirements. As a result, the ability of CTA to detect transients, without a monitoring facility, can be seriously affected. The existence of a monitoring instrument with the quoted SWGO performance would lead to the recovery of a significant fraction of the longest-duration triggers and, possibly, achieve even better results on the shortest ones. This strategy, therefore, would represent a viable system to trigger CTA observations on the most relevant VHE transient events and also to collect independent data, extending our ability to monitor VHE activity towards sources that lie at $z \approx 0.3$ and possibly beyond.

5 CONCLUSIONS

The study of VHE transient phenomena is growing in importance, now that flaring activity in blazars has been shown to contribute to the acceleration of ultra-energetic particles and that VHE photons from GRBs have been firmly detected. In this work, we analysed the results of the γ-ray monitoring campaign carried out by the *Fermi*-LAT instrument in order to identify the sources of flaring activity that are most likely associated with transient VHE emission. We estimated the expected fluxes of these VHE transients and compared them with the predicted performance of CTA-S and of monitoring facilities such as LHAASO and SWGO. We pointed out that some of the selected sources are expected to have strong enough flaring activity to be tracked by EAS arrays that continuously scan wide portions of the sky. We showed that instruments with optimized sub-TeV capabilities are able to provide relevant information on a substantial fraction of events that CTA could detect only if properly triggered. At present, most of the triggers are provided by satellites at relatively low energy, while the high-energy information only comes with some delay (for instance, it takes approximately 6 hr before LAT data can be processed). EAS arrays, on the other hand, can directly trigger on the VHE band, with shorter response times. Given that EAS arrays can cover very large instrumented surfaces at a relatively low cost and that they have the further advantage that they can be maintained and upgraded, compared with a space mission, we point out that obtaining good sensitivities to the sub-TeV range of these detectors will bring major improvements in the role of VHE transients as cosmic messengers.

[4]https://www.cta-observatory.org/science/cta-performance/

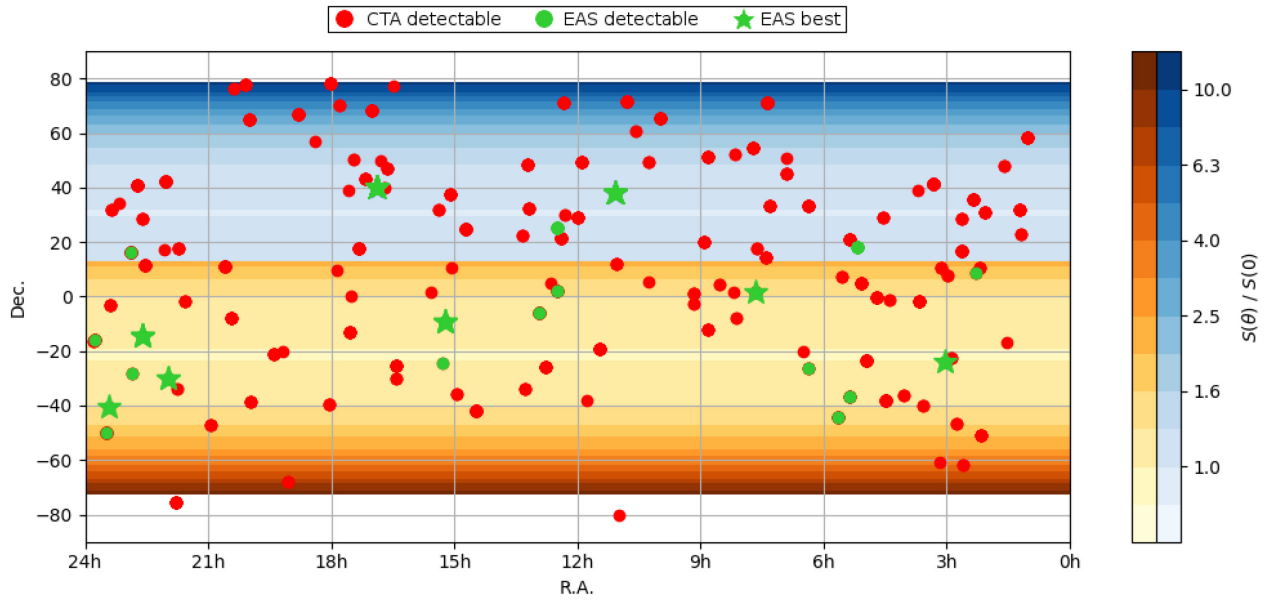

Figure 3. Distribution of VHE flaring blazars, compared with the sky coverage of LHAASO (blue shaded region) and SWGO (orange shaded region) within a FoV of 50º from zenith, assuming a SWGO site with latitude 23ºS. The colour shading represents the sensitivity degradation with respect to a source that culminates at the zenith. The sensitivity comparison in the overlap region is computed at 300 GeV, and only the instrument with the best estimated performance is plotted. The red dots represent objects for which *Fermi*-LAT detected flares that would be bright enough to be observed by CTA in 1 hr, but are too faint for the computed EAS sensitivities. The green dots are sources whose flares are comparable to the sensitivity of the relevant monitoring instrument, while the stars represent objects whose flares either have already been detected by HAWC, or their *Fermi*-LAT spectral fit is significantly brighter than the predicted EAS sensitivity limit scaled down to the duration of the flare. Every source can produce more than one flare.

Table 1. List of AGNs that have been detected by *Fermi*-LAT with an energy flux greater than 10^{-12} erg cm^{-2} s^{-1} above 10 GeV and associated with flaring activity above the sensitivity limit of the monitoring facilities. The columns report the name of the AGN, its 3FHL association, the sky coordinates (right ascension and declination, J2000), the redshift, the number of associated flares in 7.4 yr, a flag stating whether the source is listed in *TeVCat*, and the energy flux obtained from a power-law fit to the 3FHL data. Names in bold-face denote flares that are significantly stronger than the corresponding detection limit (marked with stars in Fig. 3).

Name	3FHL source	R.A. [hh:mm:ss]	Dec. [dd:mm:ss]	z	$N_{\rm flares}$	*TeVCat*	3FHL en. flux [10^{-12} erg cm^{-2} s^{-1}]
TXS 0214+083	J0217.1+0836	02: 17: 17.12	+08: 37: 03.89	0.085	2	N	2.248 ± 0.789
PKS 0301–243	J0303.4–2407	03: 03: 26.50	−24: 07: 11.42	0.260	3	Y	36.892 ± 4.831
PKS 0507+17	J0510.0+1800	05: 10: 02.37	+18: 00: 41.58	0.416	9	N	5.191 ± 1.034
PKS 0521–365	J0523.0–3627	05: 22: 57.98	−36: 27: 30.85	0.055	11	N	5.520 ± 1.610
PKS 0537–441	J0538.8–4405	05: 38: 50.36	−44: 05: 08.94	0.892	91	N	37.847 ± 2.540
PMN J0622–2605	J0622.4–2606	06: 22: 22.06	−26: 05: 44.64	0.414	3	N	11.495 ± 2.740
PKS 0736+0174	J0739.3+0137	07: 39: 18.03	+01: 37: 04.62	0.191	33	Y	2.986 ± 1.039
MRK 421	J1104.4+3812	11: 04: 27.31	+38: 12: 31.80	0.031	9	Y	437.000 ± 18.600
3C 273	J1229.2+0201	12: 29: 06.70	+02: 03: 08.60	0.158	66	N	1.309 ± 0.496
ON 246	J1230.2+2517	12: 30: 14.09	+25: 18: 07.14	0.135	18	Y	8.428 ± 1.621
3C 279	J1256.1–0547	12: 56: 11.17	−05: 47: 21.53	0.536	79	Y	18.588 ± 2.200
PKS 1510–089	J1512.8–0906	15: 12: 50.53	−09: 05: 59.83	0.360	187	Y	35.061 ± 3.116
Ap Librae	J1517.6–2422	15: 17: 41.81	−24: 22: 19.48	0.049	1	Y	20.327 ± 3.354
MRK 501	J1653.8+3945	16: 53: 52.22	+39: 45: 36.61	0.033	2	Y	156.000 ± 11.000
PKS 2155–304	J2158.8–3013	21: 58: 52.06	−30: 13: 32.12	0.116	3	Y	132.957 ± 8.901
PKS 2233–148	J2236.5–1433	22: 36: 34.09	−14: 33: 22.19	0.325	17	N	9.309 ± 1.620
PMN J2250–2806	J2250.7–2806	22: 50: 44.49	−28: 06: 39.32	0.525	6	N	4.811 ± 1.104
3C 454.3	J2253.9+1608	22: 53: 57.75	+16: 08: 53.56	0.859	301	N	32.758 ± 2.202
1ES 2322–40.9	J2324.7–4040	23: 24: 44.67	−40: 40: 49.44	0.174	1	N	9.439 ± 2.197
PKS 2326–502	J2329.2–4955	23: 29: 20.88	−49: 55: 40.64	0.518	76	N	7.931 ± 0.993
PMN J2345–1555	J2345.1–1554	23: 45: 12.56	−15: 55: 07.83	0.621	34	N	2.027 ± 0.656

ACKNOWLEDGEMENTS

The authors would like to thank F. Longo, N. Omodei and the referee for useful discussions and suggestions.

This work was partly performed under project PTDC/FIS-PAR/29158/2017, Fundação para a Ciência e Tecnologia. RC is grateful for financial support from OE – Portugal, FCT, I. P., under DL57/2016/cP1330/cT0002.

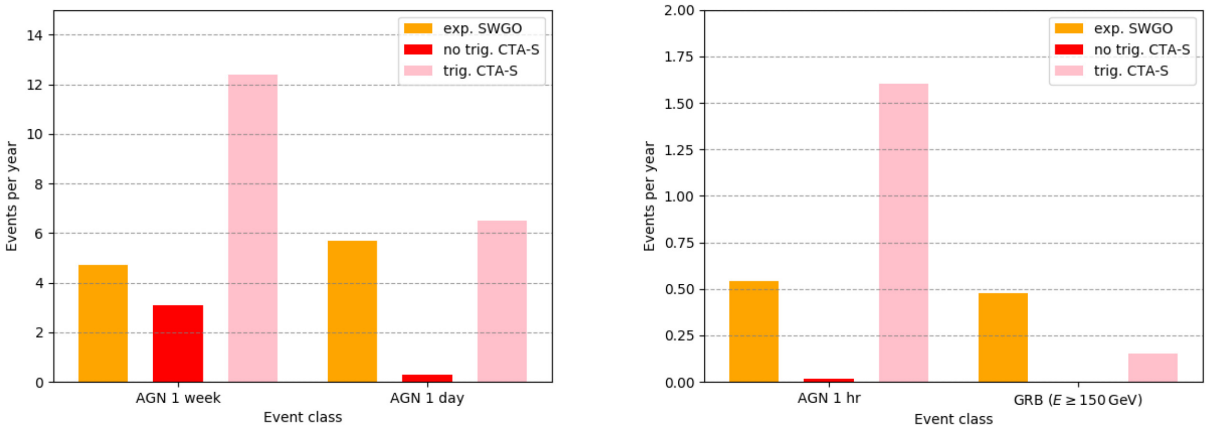

Figure 4. Histograms illustrating the predicted detection rates of VHE transients after 1 yr of observations with SWGO and CTA-S. The colour bars represent the expected rates at which VHE transients can be detected by SWGO (yellow), CTA-S without a trigger (red), and CTA-S assuming a perfect monitoring program that issues triggers for all VHE transients (pink). The analysis takes into account the instrument sensitivities, duty cycles and FoVs, and divides the transients into long events, for which the transit over the observing site is granted (left panel), and short events, where the additional possibility that the transient is in an unobservable portion of the sky is taken into account (right panel). To estimate the CTA serendipitous detection rate, we assume that the area scanned by CTA increases with the duration of the flare as a result of the combination of different pointings.

The *Fermi*-LAT Collaboration acknowledges generous ongoing support from a number of agencies and institutes that have supported both the development and the operation of the LAT as well as scientific data analysis. These include the National Aeronautics and Space Administration and the Department of Energy in the United States, the Commissariat à l'Energie Atomique and the Centre National de la Recherche Scientifique / Institut National de Physique Nucléaire et de Physique des Particules in France, the Agenzia Spaziale Italiana and the Istituto Nazionale di Fisica Nucleare in Italy, the Ministry of Education, Culture, Sports, Science and Technology (MEXT), High Energy Accelerator Research Organization (KEK) and Japan Aerospace Exploration Agency (JAXA) in Japan, and the K. A. Wallenberg Foundation, the Swedish Research Council and the Swedish National Space Agency in Sweden.

This research has made use of the CTA instrument response functions provided by the CTA Consortium and Observatory: see https://www.ctaobservatory.org/science/cta-performance/ (version prod3b-v2) for more details.

Additional support for science analysis during the operations phase from the Istituto Nazionale di Astrofisica in Italy and the Centre National d'Études Spatiales in France is gratefully acknowledged. This work was carried out in part under DOE Contract DEAC02-76SF00515.

DATA AVAILABILITY

There are no new data associated with this article.

REFERENCES

Abbott B. P. et al., 2017a, ApJ, 848, L12
Abbott B. P. et al., 2017b, ApJ, 848, L13
Abdalla H. et al., 2019, Nature, 575, 464
Abdollahi S. et al., 2017, ApJ, 846, 34
Abeysekara A. U. et al., 2018, ApJ, 861, L20
Actis M. et al., 2011, Exp. Astron., 32, 193
Agostinelli S. et al., 2003, Nucl. Instrum. Meth., A506, 250
Aharonian F. et al., 2006, A&A, 457, 899
Ajello M. et al., 2017, ApJS, 232, 18
Ajello M. et al., 2019, ApJ, 878, 52
Albert A. et al., 2019, preprint (arXiv:1902.08429)
Aleksić J. et al., 2016, Astropart. Phys., 72, 61
Anderhub H. et al., 2013, J. Instrum., 8, P06008
Assis P. et al., 2018, Astropart. Phys., 99, 34
Atwood W. B. et al., 2009, ApJ, 697, 1071
Bernardini M. G., Bissaldi E., Bosnjak Z., Carosi A., D'Avanzo P., Di Girolamo T., Inoue S., Gasparetto T., 2019, in Gupta S., ed., 36th Int. Cosmic Ray Conf. (ICRC2019), SISSA, Medialab, Madison, WI, p. 598
Blanchard P. K. et al., 2017, ApJ, 848, L22
Cowperthwaite P. S. et al., 2017, ApJ, 848, L17
CTA Consortium, 2019, Science with the Cherenkov Telescope Array, World Scientific Publishing Co. Pte. Ltd., Singapore
Desai A., Helgason K., Ajello M., Paliya V., Domínguez A., Finke J., Hartmann D., 2019, ApJ, 874, L7
DeYoung T., 2012, Nuclear Instrum. Methods Phys. Res. A, 692, 72
Di Sciascio G., LHAASO Collaboration, 2016, Nuclear Part. Phys. Proc., 279, 166
Domínguez A. et al., 2011, MNRAS, 410, 2556
Fermi-LAT Collaboration, 2020, ApJS, 247, 33
Galli A., Piro L., 2008, A&A, 489, 1073
HESS Collaboration, 2017, A&A, 600, A89
Heck D., Knapp J., Capdevielle J. N., Schatz G., Thouw T., 1998, CORSIKA: A Monte Carlo Code to Simulate Extensive Air Showers, Forschungszentrum Karlsruhe, Karlsruhe, Germany
Holder J. et al., 2008, in Aharonian F. A., Hofmann W., Rieger F., eds, AIP Conf. Ser. Vol. 1085,, American Institute of Physics, 4th International Meeting on High Energy Gamma-ray Astronomy, Heidelberg, Germany, p. 657
IceCube Collaboration, 2018, Science, 361, eaat1378
Kudoda A. M., Faltenbacher A., 2017, MNRAS, 467, 2896
MAGIC Collaboration, 2019, Nature, 575, 455
Meegan C. et al., 2009, ApJ, 702, 791
Mirzoyan R., 2017, Astron. Telegram, 10817
Mirzoyan R., 2019, Astron. Telegram, 12390
Paiano S., Falomo R., Treves A., Scarpa R., 2018, ApJ, 854, L32
Prince R., Majumdar P., Gupta N., 2017, ApJ, 844, 62
Schoorlemmer H., 2019, in Gupta S., ed., 36th Int. Cosmic Ray Conf. (ICRC2019), Sissa Medialab, Madison; WI, p. 785, preprint (arXiv:1908.08858)
Wakely S. P., Horan D., 2008, International Cosmic Ray Conference, 3, 1341
Zacharias M. et al., 2019, Galaxies, 7, 41

This paper has been typeset from a TEX/LATEX file prepared by the author.